Tafamidis, a potent and selective transthyretin kinetic stabilizer that inhibits the amyloid cascade

Christine E. Bulawa[a,1], Stephen Connelly[b], Michael DeVit[c], Lan Wang[d], Charlotte Weigel[a], James A. Fleming[a], Jeff Packman[c], Evan T. Powers[e,f], R. Luke Wiseman[g], Theodore R. Foss[h], Ian A. Wilson[b,f], Jeffery W. Kelly[e,f,g], and Richard Labaudinière[c]

[a]Pfizer Orphan and Genetic Diseases Research Unit, Cambridge, MA 02140; [b]Department of Molecular Biology, The Scripps Research Institute, La Jolla, CA 92037; [c]FoldRx Pharmaceuticals, a wholly-owned subsidiary of Pfizer, Cambridge, MA 02140; [d]Cardiovascular and Metabolic Diseases, Novartis Institutes for BioMedical Research, Cambridge, MA 02139; [e]Department of Chemistry, The Scripps Research Institute and [f]The Skaggs Institute for Chemical Biology, La Jolla, CA 92037; [g]Department of Molecular and Experimental Medicine, The Scripps Research Institute, La Jolla, CA 92037; and [h]Life Technologies, Genetic Systems, Beverly, MA 01915

Edited by Carl Frieden, Washington University School of Medicine, St. Louis, MO, and approved April 23, 2012 (received for review January 3, 2012)

The transthyretin amyloidoses (ATTR) are invariably fatal diseases characterized by progressive neuropathy and/or cardiomyopathy. ATTR are caused by aggregation of transthyretin (TTR), a natively tetrameric protein involved in the transport of thyroxine and the vitamin A–retinol-binding protein complex. Mutations within TTR that cause autosomal dominant forms of disease facilitate tetramer dissociation, monomer misfolding, and aggregation, although wild-type TTR can also form amyloid fibrils in elderly patients. Because tetramer dissociation is the rate-limiting step in TTR amyloidogenesis, targeted therapies have focused on small molecules that kinetically stabilize the tetramer, inhibiting TTR amyloid fibril formation. One such compound, tafamidis meglumine (Fx-1006A), has recently completed Phase II/III trials for the treatment of Transthyretin Type Familial Amyloid Polyneuropathy (TTR-FAP) and demonstrated a slowing of disease progression in patients heterozygous for the V30M TTR mutation. Herein we describe the molecular and structural basis of TTR tetramer stabilization by tafamidis. Tafamidis binds selectively and with negative cooperativity (K_ds ∼2 nM and ∼200 nM) to the two normally unoccupied thyroxine-binding sites of the tetramer, and kinetically stabilizes TTR. Patient-derived amyloidogenic variants of TTR, including kinetically and thermodynamically less stable mutants, are also stabilized by tafamidis binding. The crystal structure of tafamidis-bound TTR suggests that binding stabilizes the weaker dimer-dimer interface against dissociation, the rate-limiting step of amyloidogenesis.

drug | aggregation inhibition

Amyloid diseases appear to be caused by the extracellular accumulation of protein aggregates, including cross–β-sheet amyloid fibrils for which these maladies are named (1–3). Wild-type (WT) and/or mutant transthyretin (TTR) amyloidogenesis leads to the TTR amyloidoses (ATTR), with phenotypes including peripheral neuropathy (4, 5) and/or cardiomyopathy (6, 7). ATTR are progressive and fatal within 10 y of onset. The most common mutations are V30M, which causes familial amyloid polyneuropathy (TTR-FAP) (8), and V122I, which causes familial amyloid cardiomyopathy (TTR-CM) (9). In the elderly, WT-TTR amyloidogenesis leads to the cardiomyopathy called senile systemic amyloidosis (SSA) (6, 7).

Homotetrameric WT-TTR comprises 127-amino-acid, β-sheet–rich subunits and is made primarily by the liver, which secretes it into the blood, where it binds to and carries holo retinol-binding protein (10, 11). The native state of TTR features two largely unoccupied thyroxine (T_4)-binding sites (Fig. 1) that are generated by the weaker dimer–dimer interface of TTR (12–15). Rate-limiting tetramer dissociation about this interface generates dimers that rapidly dissociate into monomers (14, 16, 17). Partial monomer unfolding, likely involving β-strand dissociation (18), promotes misassembly into soluble oligomers and amyloid fibrils through a thermodynamically favorable downhill process (15, 19). Misfolded monomers and oligomers have been implicated as neurotoxic species (20–23). Disease-associated mutations destabilize the TTR tetramer and some increase the velocity of rate-limiting tetramer dissociation (17, 24–26).

In populations of Portuguese descent, inheritance of one copy of V30M TTR typically leads to TTR-FAP with high clinical penetrance; however, a few V30M carriers develop mild pathology or no disease. These carriers have a different mutation, T119M, on their second TTR allele (27), resulting in the formation of T119M/V30M heterotetramers, which are more stable than heterotetramers comprising V30M and WT subunits (17, 28, 29). Tetramer dissociation is slowed proportional to the number of T119M subunits in the heterotetramer, due to destabilization of the dissociative transition state (17). Therefore, increasing the kinetic barrier for tetramer dissociation, which is the initial and rate-limiting step of TTR amyloidogenesis, is the likely mechanism by which T119M prevents TTR-FAP in V30M/T119M compound heterozygotes (17, 28).

Because lowering the native state energy through small-molecule binding to the TTR tetramer also increases the activation energy associated with tetramer dissociation (15, 17, 30–33), a mechanism known to ameliorate TTR-FAP based on the T119M interallelic trans suppression data, we predicted that small-molecule TTR kinetic stabilizers (amyloid inhibitors) would be disease-modifying therapies for ATTR (15, 17).

Of the multiple TTR kinetic stabilizer structures reported (15, 30–32, 34–45), the benzoxazoles (32) were pursued to identify an orally bioavailable candidate exhibiting potent and selective TTR binding in blood, while lacking nonsteroidal antiinflammatory (NSAID) activity, which is contraindicated in patients with cardiomyopathy. Tafamidis, or 2-(3,5-dichloro-phenyl)-benzoxazole-6-carboxylic acid, meets all of these criteria and was selected for clinical development. Herein we show that tafamidis selectively binds TTR with negative cooperativity and kinetically

PHARMACOLOGY

Author contributions: C.E.B., S.C., M.D., E.T.P., R.L.W., J.W.K., and R.L. designed research; S.C., M.D., L.W., C.W., R.L.W., and T.R.F. performed research; C.E.B., L.W., J.F., and J.P. contributed new reagents/analytic tools; C.E.B., S.C., M.D., L.W., C.W., J.F., J.P., E.T.P., R.L.W., T.R.F., I.A.W., and R.L. analyzed data; and C.E.B., S.C., E.T.P., R.L.W., I.A.W., J.W.K., and R.L. wrote the paper.

Conflict of interest statement: J.W.K. is a founder, consultant to, and shareholder of FoldRx Pharmaceuticals, which was acquired by Pfizer, Inc. in October 2010. At the time of manuscript development, C.E.B., M.D., L.W., C.W., J.F., J.P., and R.L. were full-time employees of FoldRx Pharmaceuticals. E.T.P. has received license fees and royalties from Pfizer related to tafamidis patents. S.C., R.L.W., I.A.W., and T.R.F. have no conflicts of interest to disclose.

This article is a PNAS Direct Submission.

Freely available online through the PNAS open access option.

Data deposition: The atomic coordinates have been deposited in the Protein Data Bank, www.pdb.org (PDB ID code 3TCT).

[1]To whom correspondence should be addressed. E-mail: Christine.Bulawa@pfizer.com.

This article contains supporting information online at www.pnas.org/lookup/suppl/doi:10.1073/pnas.1121005109/-/DCSupplemental.

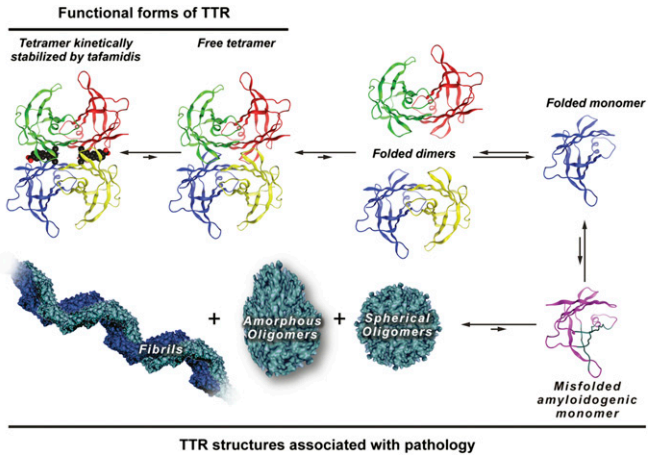

Fig. 1. The TTR amyloid cascade. Amyloid formation by TTR requires rate-limiting tetramer dissociation to a pair of folded dimers, which then quickly dissociate into folded monomers. Partial unfolding of the monomers yields the aggregation-prone amyloidogenic intermediate. The amyloidogenic intermediate of TTR (*Lower Right*) retains much of its native structure (shown in purple), probably with some β-strand dissociation (shown in turquoise). The amyloidogenic intermediate can misassemble to form a variety of aggregate morphologies, including spherical oligomers, amorphous aggregates, and fibrils. Tafamidis binding to the TTR tetramer (*Upper Left*) dramatically slows dissociation, thereby efficiently inhibiting aggregation.

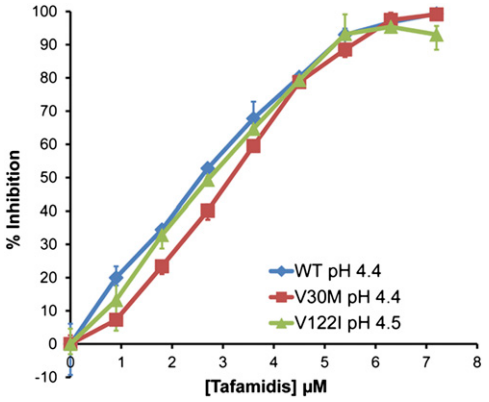

Fig. 2. Inhibition of WT, V30M, and V122I TTR fibril formation under acidic conditions after 72 h. Purified TTR homotetramers (WT, V30M, or V122I at 3.6 μM) were mixed with tafamidis at final concentrations of 0, 0.9, 1.8, 2.7, 3.6, 4.5, 5.4, 6.3, and 7.2 μM and then incubated for 30 min at 25 °C. The pH was then adjusted to 4.4 (WT and V30M) or 4.5 (V122I) to allow for stabilization by tafamidis to be tested under conditions of comparable kinetics of fibril formation for the three alleles. The samples were incubated at 37 °C for 72 h and turbidity was then measured at 350 and 400 nm using a UV-visible (vis) spectrometer. For each allele, the endpoint turbidity in the absence of tafamidis (which varies slightly by allele) was defined as 100% fibril formation. Therefore, 5% fibril formation corresponds to a compound inhibiting 95% of TTR fibril formation after 72 h (60). Error bars represent the minimum and maximum values from three technical replicates.

stabilizes WT-TTR and mutant tetramers under denaturing and physiologic conditions, inhibiting amyloidogenesis. A high-resolution crystal structure reveals the details of how tafamidis binds to the weaker dimer–dimer interface of TTR.

Results

Tafamidis Stabilizes TTR Under Fibril-Promoting Conditions. Incubation of WT or mutant TTR homotetramers (3.6 μM) at a pH of 4.4–4.5 over 72 h results in tetramer dissociation, partial monomer denaturation, and misassembly into amyloid fibrils and other aggregates (Fig. 1) (19, 46). Purified WT, V30M, and V122I homotetramers were incubated with tafamidis at concentrations ranging from 0 to 7.2 μM. The pH was adjusted to either 4.4 or 4.5 to promote an identical rate of amyloidogenesis among these sequences (without tafamidis). After 72 h (aggregation is complete without tafamidis), amyloidogenesis was quantified by measuring turbidity at 350 and 400 nm (16). Consistent with previous studies (32), tafamidis dose-dependently inhibited WT-TTR amyloidogenesis (Fig. 2). Importantly, this study shows that tafamidis stabilized the two most clinically significant amyloidogenic mutant homotetramers, V30M-TTR and V122I-TTR, with potency and efficacy comparable to that of WT-TTR (Fig. 2). Tafamidis reached its half-maximal effective concentration (EC_{50}) at a tafamidis:TTR tetramer molar ratio of <1 (EC_{50} of 2.7–3.2 μM, corresponding to a tafamidis:TTR molar ratio of 0.75–0.90). Under these conditions, the occupancy of less than one binding site of TTR by tafamidis reduces TTR fibril formation by 50%, consistent with reports that binding to only one T_4-binding site is sufficient to kinetically stabilize tetrameric TTR (33).

Tafamidis Kinetically Stabilizes TTR Under Denaturing Conditions. The TTR tetramer must dissociate before urea can unfold its β-sheet–rich tertiary structure (47). Therefore, at high urea concentrations, the rate of tetramer dissociation is linked irreversibly to fast monomer unfolding, which is easily followed by far UV circular dichroism spectroscopy (14, 24, 25, 33). TTR (1.8 μM) was incubated together with tafamidis (tafamidis:TTR tetramer molar ratios of 0, 1, and 2) and urea (6.5 M final concentration) to denature any monomer that is produced, and circular dichroism spectra were collected at 0 and 72 h (the time required for maximum denaturation without tafamidis). As shown in Fig. 3, only 33% of the TTR tetramer dissociates after a 72-h period at a tafamidis:TTR tetramer molar ratio of 1 and less than 3% of tetramers dissociate when tafamidis is used at twice the concentration of TTR, indicating dose-dependent kinetic stabilization of the tetramer.

Tafamidis Kinetically Stabilizes TTR Under Physiologic Conditions. It is difficult to detect folded monomeric or misfolded monomeric TTR upon dissociation from the tetramer under physiologic conditions. However, it is possible to indirectly detect monomer formation by using subunit exchange experiments (28, 48, 49). It was previously demonstrated that tetramer dissociation is rate limiting for subunit exchange, that the tetramer dissociates to monomers through transient dimers on a biologically relevant

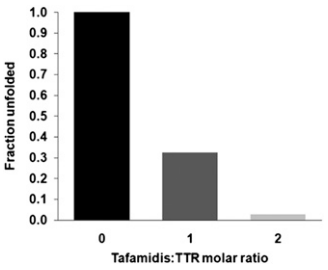

Fig. 3. Tafamidis stabilizes WT-TTR to urea-mediated denaturation. WT-TTR (1.8 μM) was incubated with 0, 1.8, and 3.6 μM tafamidis (corresponding to TTR:tafamidis molar ratios of 0, 1, and 2). Denaturation was initiated by adding urea to a final concentration of 6.5 M. After 72 h, circular dichroism spectra were collected between 220 and 213 nm, with scanning every 0.5 nm and an averaging time of 10 s. Each wavelength was scanned once. The values for the amplitude were averaged between 220 and 213 nm to determine the extent of β-sheet loss throughout the experiment. Results were expressed as a percentage of fraction unfolded relative to the amount observed in the absence of tafamidis (17).

timescale, and that folded monomers reassociate to form mixed tetramers under nondenaturing conditions (14, 48, 49). To study subunit exchange, two homotetramers were used. One was composed of WT-TTR subunits that were labeled at the N terminus with a negatively charged FLAG-tag (Fig. 4*A*, 4 FLAG). The other was made up of untagged WT subunits (Fig. 4*A*, 0 FLAG). After these tetramers were mixed, time-dependent subunit exchange between them could be quantified in buffers at physiologic pH using ion-exchange chromatography (48). A TTR kinetic stabilizer such as tafamidis is expected to decrease the rate of tetramer dissociation, which would slow subunit exchange between the WT-TTR homotetramer and FLAG-tagged WT-TTR homotetramer. When subunit exchange is complete, the monomers are statistically distributed, with tetramers 0 FLAG, 1 FLAG, 2 FLAG, 3 FLAG, and 4 FLAG being present in a ratio of 1:4:6:4:1. Because each FLAG tag adds approximately six negative charges to each TTR subunit, the more FLAG-tag TTR subunits in the tetramer, the longer the retention time on an anion exchange column, allowing separation of all five tetramers and quantification of the extent of exchange as a function of time (48).

Solutions of homotetrameric WT-TTR (0 FLAG, 1.8 μM) and homotetrameric WT-TTR bearing an N-terminal acidic FLAG tag (4 FLAG WT-TTR; 1.8 μM) were each individually preincubated with tafamidis as a function of concentration (tafamidis:TTR tetramer molar ratios of 0, 0.25, 0.50, 0.75, 1.00, 1.25, and 1.50). The subunit exchange reaction was initiated by mixing the homotetramers (25 °C; pH 7), and exchange was quantified by anion-exchange chromatography over the course of 8 d (except for the tafamidis:TTR tetramer molar ratio of 1.50, which was studied for 11 d). The exchange was complete in the vehicle control (Fig. 4*A*, gray line) after 96 h of incubation as shown by the statistical distribution of subunits. In the presence of tafamidis (tafamidis:TTR tetramer molar ratio of 1.50), negligible tetramer dissociation was observed after 96 h (Fig. 4*A*, black line), with a calculated fraction exchange of <5% (Fig. 4*B*, orange line), and after 11 d the fraction of exchange was still <10%. At a molar ratio of 1.25, <20% subunit exchange was observed after 96 h. Even at a molar ratio of 1, the fraction of exchange was only 15% after 24 h (70% was exchanged in the absence of tafamidis). Stabilization over this period is highly relevant because the TTR half-life in plasma is 24 h. Collectively, these data demonstrate that tafamidis dose-dependently decreases the rate of tetramer dissociation at physiologic pH.

Tafamidis Binds with High Affinity to TTR at Its T_4-Binding Sites. We used two methods to determine the binding constants of tafamidis to WT-TTR. The first employs a modeling analysis of the subunit exchange time courses (Fig. 4*B*) at neutral pH as a function of tafamidis concentration (49). The appearance of the various mixed tetramers and the disappearance of the homotetramers appear to be simple unimolecular processes with the same apparent rate constant, k_{app}, which is equal to the tetramer dissociation rate constant, k_{diss}, in the absence of ligands (49). As TTR cannot exchange subunits when the tetramer is bound to a ligand (33, 49), $k_{app} = f_{unbound} \times k_{diss}$ in the presence of ligands, where $f_{unbound}$ is the fraction of TTR tetramers that do not have bound ligands.

Fitting the data in Fig. 4*B* to a single exponential and dividing the resulting k_{app} values by k_{diss} gave $f_{unbound}$ at a series of tafamidis concentrations. These $f_{unbound}$ vs. ligand concentration data were then fit with a second-order binding polynomial (50) to determine K_{d1} = 2 nM and K_{d2} = 154 nM, the dissociation constants for the first and second binding sites of TTR (49).

Isothermal titration calorimetry (ITC) was also used to determine the binding constants of tafamidis to TTR (45). A solution of tafamidis was titrated into an ITC cell containing WT-TTR (17 μM) in identical buffers. The initial 2.5-μL injection of tafamidis (500 μM) was followed by forty-nine 5-μL injections (25 °C), and the heat evolved was measured as a function of time after each injection. After subtracting the blank, the area underneath each injection peak was integrated, corresponding to

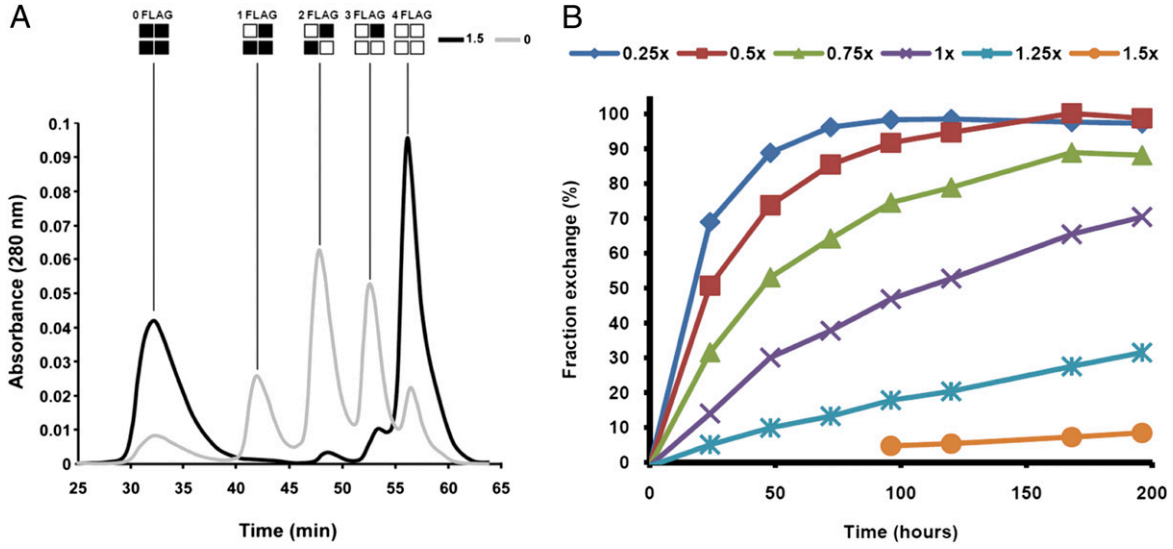

Fig. 4. Subunit exchange between WT-TTR and FLAG-tagged WT-TTR under physiologic conditions, monitored by anion exchange chromatography. Black square, WT-TTR; white square, FLAG-tagged WT-TTR. Homotetramers of WT-TTR (0 FLAG; 1.8 μM) and WT-TTR tagged with an N-terminal acidic FLAG tag (4 FLAG; 1.8 μM) were mixed with tafamidis at different concentrations (tafamidis:TTR tetramer molar ratios: 0.25, 0.50, 0.75, 1.00, 1.25, and 1.50) and incubated at 25 °C at a pH of 7. Samples were analyzed by anion exchange chromatography at the indicated times. (*A*) FPLC trace after 96-h incubation of 0 Flag TTR with 4 Flag TTR in the absence (gray) or presence (black) of tafamidis at a tafamidis:TTR tetramer molar ratio of 1.5. (*B*) Dose-dependent stabilization of TTR by tafamidis. At each time point, the extent of exchange was calculated by dividing the peak area of each tetramer by the sum of the peak areas for all of the tetramers. The fraction exchange was calculated by dividing the extent of exchange of 2 FLAG at each data point by 0.375 multiplied by 100. The predicted complete extent of exchange for 2 FLAG is 0.375, based on the statistical distribution of 1:4:6:4:1 for tetramer 0 FLAG–4 FLAG, respectively. Values for samples of tafamidis:TTR tetramer molar ratio = 1.5 at 220 and 264 h (not shown) were 9.5% and 9.8%, respectively.

total heat released for that injection (*SI Appendix*, Fig. S1*A*). This integrated heat was plotted against the molar ratio of tafamidis added to TTR in the cell, yielding a complete binding isotherm (*SI Appendix*, Fig. S1*B*). This isotherm was best fit by a model in which tafamidis binds to TTR with negative cooperativity, with K_{d1} = 3 nM and K_{d2} = 278 nM. Although the aforementioned methods disagree somewhat on the determination of K_{d2}, a difference of a factor of 2 in equilibrium constant equates to a difference of only ∼0.4 kcal/mol at room temperature. So in terms of energy, the agreement is quite good.

Tafamidis Stabilizes the Weaker TTR Dimer–Dimer Interface. The crystal structure of WT-TTR bound by tafamidis was determined to 1.3 Å resolution by cocrystallization (tafamidis:TTR tetramer molar ratio of 5.1) at a pH of 5.5 (*SI Appendix*, Table S1). To date, this is the highest-resolution TTR:ligand structure solved, allowing for the unambiguous placement of tafamidis in the $2F_o$–F_c electron density maps (41) (Fig. 5). The 3,5-dichloro substituents occupy the two symmetrical halogen-binding pockets (HBPs), 3 and 3′, which are located in the inner binding cavity (Fig. 5*B*). The benzoxazole ring of tafamidis is positioned in the hydrophobic environment of HBP2 and -2′ and HBP1 and -1′. In this orientation, the *meta*-carboxylate substituent on the benzoxazole extends out into the periphery of the T_4-binding site, where it engages in water-mediated H-bonds with the Lys15/15′ and Glu54/54′ residues of TTR. Because these low B-value waters are not conserved in other TTR apo structures or ligand$_2$•TTR structures and because these H-bonds are solvated, we do not anticipate that they are a driving force for tafamidis binding to TTR, but rather a consequence of binding. This combination of hydrophobic and ionic interactions appears to bridge adjacent dimers to kinetically stabilize the TTR tetramer (14, 15, 34).

Tafamidis Binds Selectively to TTR in Human Plasma. We next examined the relative binding selectivity of tafamidis for TTR compared with the ∼4,000 additional proteins in plasma. Tafamidis (7.2 μM) was incubated with human plasma (3.6 μM TTR) overnight; TTR and any bound tafamidis were then immunocaptured using a resin-bound polyclonal antibody to TTR (51). After washing the immobilized TTR, we liberated the TTR–tafamidis complex from the resin with triethylamine and determined the stoichiometry of tafamidis relative to TTR by reverse-phase HPLC analysis (51). Under these conditions, tafamidis exhibits a binding stoichiometry of 0.81 ± 0.02 (*SI Appendix*, Fig. S2), confirming previous results (32). Because several wash steps were used, likely resulting in tafamidis loss (52), the stoichiometry determined should be considered a lower limit.

Tafamidis Stabilizes WT, V30M, and V122I TTR in Human Plasma. WT, V30M, and V122I TTR were evaluated because these sequences are linked to SSA and the majority of TTR-FAP and TTR-CM cases, respectively. To assess kinetic stabilization, tafamidis was preincubated with plasma samples, and urea (4.8 M) was added as a denaturation stress. After 1, 2, 3, and 4 d, aliquots were withdrawn and treated with glutaraldehyde to cross-link the TTR tetramer remaining (53). Samples were then analyzed by SDS/PAGE, followed by Western blotting using anti-TTR antiserum to measure the remaining amount of TTR tetramer. When the TTR monomer is unfolded in 4.8 M urea, it is heavily modified by glutaraldehyde, such that it is no longer recognized by the TTR antibody (53).

A human plasma sample from a healthy volunteer exhibited nearly complete WT-TTR denaturation by day 3 of incubation in the absence of tafamidis, and complete denaturation after 4 d (Fig. 6*A*). In the presence of 3.6, 5.4, and 7.2 μM tafamidis (corresponding to tafamidis:TTR tetramer molar ratios of ∼1.0, 1.5, and 2.0, respectively) dose-dependent stabilization is observed even after 4 d (Fig. 6*A*). Tafamidis (7.2 μM) also strongly stabilized TTR heterotetramers containing WT and mutant subunits in plasma samples from patients carrying V30M or V122I mutations (Fig. 6 *B* and *C*). These ex-vivo results demonstrate the efficacy of a 7.2-μM tafamidis dose to stabilize a variety of TTR tetramers in the presence of urea (strongly denaturing), even though urea likely lowers the binding affinity of tafamidis to TTR.

TTR stabilization in plasma was also observed by using a modification of the method described above, in which the Western blotting was replaced by an immunoturbidity measurement (54), a readout that is amenable to automation used in clinical laboratories. The large antibody–TTR tetramer complexes that self-assemble precipitate out of solution; thus, the amount of turbidity can be used to quantify the TTR tetramer as the heavily glutaraldehyde-modified TTR monomer is not detected by the antibody (53). Preincubation with tafamidis stabilized TTR in a dose-dependent manner, similar to that observed with Western blotting (*SI Appendix*, Fig. S3 *A* and *B*).

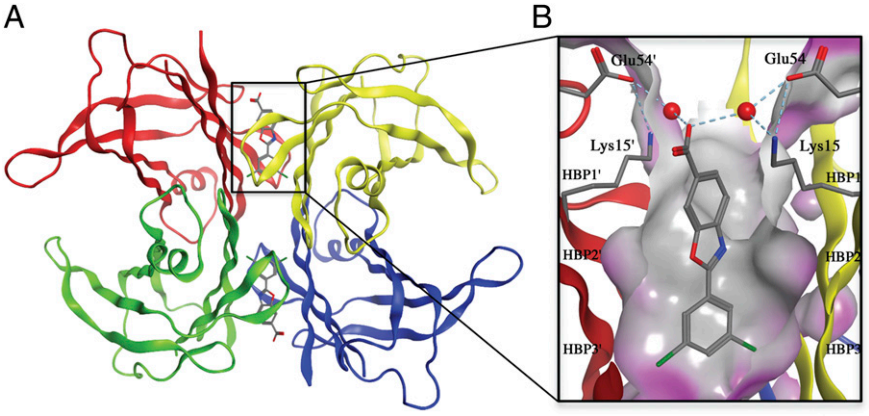

Fig. 5. Crystal structure of tafamidis bound to TTR. The coordinates are available in the Protein Data Bank under accession code 3TCT. (*A*) 3D ribbon diagram depiction of the TTR tetramer with tafamidis bound. The four TTR monomers are individually colored. (*B*) Magnified image of tafamidis bound in one of the T_4-binding sites. Connolly analytical surface representation (translucent gray, hydrophobic; translucent purple, polar) depicts the hydrophobicity of the binding site. The 3,5-chloro groups are placed in the HBPs 3 and 3′ making hydrophobic interactions, whereas the carboxylate of tafamidis engages in water-mediated H-bonds with the Lys15/15′ and Glu54/54′ residues of TTR represented by dotted lines (Lys15′-water H-bond not shown owing to tafamidis orientation). Fig. 5 was generated using the software Molecular Operating Environment, MOE (Chemical Computing Group).

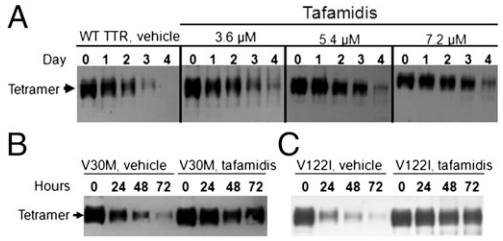

Fig. 6. Tafamidis stabilizes TTR in plasma from patients with WT, V30M, and V122I alleles under conditions of urea denaturation. (*A*) Dose-dependent stabilization of WT-TTR. Human plasma (pool, $n = 11$ healthy volunteers; Golden West Biologicals); premeasured TTR level is 3.6 μM. Under urea-mediated denaturation stress, TTR tetramer disappears over the course of 4 d. The addition of tafamidis stabilized TTR tetramer in a dose-dependent manner. Human plasma from patients with V30M TTR-FAP (*B*, $n = 4$) and V122I TTR-CM (*C*, $n = 4$) was obtained and pooled by genotype. Stabilization by tafamidis (7.2 μM) was compared with vehicle (DMSO). Tafamidis stabilized both V30M/WT and V122I/WT heterotetramers.

Tafamidis Stabilizes a Broad Range of Pathogenic TTR Variants. Plasma samples from patients harboring mutations exhibiting a wide range of kinetic and/or thermodynamic stabilities (24–26), including V30M, Y69H, F64S, I84S (lower thermodynamic stability), V122I (lower kinetic stability), and L111M (lower thermodynamic and kinetic stability), were subjected to urea denaturation, and stabilization was analyzed by immunoturbidity (except for L111M, which was analyzed by Western blot). In a broad spectrum of TTR variants, tafamidis significantly reduced the disappearance of TTR tetramer (*SI Appendix*, Fig. S4 *A* and *B*) by kinetic stabilization.

Discussion

Although fibrils are the common observable pathology in many amyloid diseases, there is a growing realization that it may be the process of amyloid fibril formation, featuring nonfibril intermediates, that actually causes proteotoxicity (55). Thus, for treatment, it is optimal to arrest the amyloid cascade (15), which is how tafamidis functions (Fig. 1). Like interallelic trans suppression, which prevents FAP onset, we showed that tafamidis, by binding to TTR, raises the energy barrier for tetramer dissociation and prevents fibril formation under both denaturing and physiologic conditions and slows TTR-FAP progression by kinetic stabilization after FAP onset (59). Tafamidis-mediated kinetic stabilization of TTR was demonstrated by slowed subunit exchange under physiologic conditions (Fig. 4) and slowed tetramer dissociation under denaturing conditions (Fig. 3).

That tafamidis occupies the T_4-binding sites in TTR raises the concern of thyroid metabolic effects; however, <1% of circulating TTR in the blood carries thyroxine because the primary carrier in blood is thyroxine-binding globulin (56–58). Consistent with these observations, tafamidis was well tolerated by patients, showing no clinically relevant effects on laboratory measures, including thyroid function (59).

Although >100 mutations at 67 sites are associated with TTR amyloidoses (60), none alter the key tafamidis-binding residues, consistent with our finding that tafamidis stabilizes five amyloidogenic variants of TTR, covering a range of energetic deficiencies. In subsequent studies, it was shown that an additional 30 amyloidogenic variants were stabilized by tafamidis, suggesting its efficacy for the vast majority of ATTR caused by TTR variants that are able to form tetramers.

In a phase II/III clinical trial of tafamidis in V30M TTR-FAP patients, this kinetic stabilizer demonstrated clinical efficacy over 18 mo of treatment. Relative to placebo controls, patients receiving tafamidis had 52% less neurologic deterioration, 53% and 80% preservation of large- and small-nerve fiber function, and improved nutritional status, outcomes that are associated with an improved quality of life (59). The tafamidis preclinical data presented within, when considered in concert with the clinical efficacy data (59), provide unique pharmacologic evidence supporting the amyloid hypothesis, the notion that lowering the efficiency of the amyloid cascade halts the degeneration of the peripheral and autonomic nervous system.

Methods

Procedures for the fibril formation assay (19, 37), immunoprecipitation of TTR: drug complexes (51), ITC (45), and urea-induced dissociation kinetics (17, 24) have been described elsewhere. Previously reported assays for compound-mediated stabilization of TTR under physiologic conditions using subunit exchange (48) or under urea denaturation stress using Western blotting (53) were performed as described. The procedure for tafamidis synthesis and complete characterization of the products (^{1}H and ^{13}C NMR spectroscopy and high-resolution mass spectra) are described in *SI Appendix*, as are the methods for X-ray crystallography and structure determination and for assaying compound-mediated stabilization of TTR by immunoturbidity.

ACKNOWLEDGMENTS. The authors thank the following investigators for generously providing plasma samples from patients with ATTR used in this study: V30M, T. Coelho (Hospital San Antonio, Porto); V122I, A. Kim and L. Bond (University of Chicago Medical Center) and D. Judge and E. Heck (The Johns Hopkins University); L111M, P. Ranløv (Hørsholm Hospital) and I. H. Svendsen (University Hospital, Copenhagen); and Y69H, F64S, and I84S, M. D. Benson (Indiana University School of Medicine). We also thank D. Grogan, C. Adams, and B. White for contributions to the manuscript and G. Dendle, S. Johnson, and D. Bosco for technical assistance. Editorial support was provided by K. Kelly (Scientific Strategy Partners) and funded by Pfizer, Inc. This study was sponsored by FoldRx Pharmaceuticals, which was acquired by Pfizer, Inc. in October 2010 and was also supported by National Institutes of Health Grants DK046335 (to J.W.K.) and CA58896 and AI42266 (to I.A.W.), as well as The Skaggs Institute (J.W.K. and I.A.W.).

1. Hardy J, Selkoe DJ (2002) The amyloid hypothesis of Alzheimer's disease: Progress and problems on the road to therapeutics. *Science* 297:353–356.
2. Taylor JP, Hardy J, Fischbeck KH (2002) Toxic proteins in neurodegenerative disease. *Science* 296:1991–1995.
3. Chiti F, Dobson CM (2006) Protein misfolding, functional amyloid, and human disease. *Annu Rev Biochem* 75:333–366.
4. Benson MD (1989) Familial amyloidotic polyneuropathy. *Trends Neurosci* 12:88–92.
5. Ando Y, Suhr OB (1998) Autonomic dysfunction in familial amyloidotic polyneuropathy (FAP). *Amyloid* 5:288–300.
6. Ng B, Connors LH, Davidoff R, Skinner M, Falk RH (2005) Senile systemic amyloidosis presenting with heart failure: A comparison with light chain-associated amyloidosis. *Arch Intern Med* 165:1425–1429.
7. Westermark P, Sletten K, Johansson B, Cornwell GG, 3rd (1990) Fibril in senile systemic amyloidosis is derived from normal transthyretin. *Proc Natl Acad Sci USA* 87:2843–2845.
8. Saraiva MJM (1995) Transthyretin mutations in health and disease. *Hum Mutat* 5:191–196.
9. Jacobson DR, et al. (1997) Variant-sequence transthyretin (isoleucine 122) in late-onset cardiac amyloidosis in black Americans. *N Engl J Med* 336:466–473.
10. Blake CC, Geisow MJ, Oatley SJ, Rérat B, Rérat C (1978) Structure of prealbumin: Secondary, tertiary and quaternary interactions determined by Fourier refinement at 1.8 A. *J Mol Biol* 121:339–356.
11. Monaco HL, Rizzi M, Coda A (1995) Structure of a complex of two plasma proteins: Transthyretin and retinol-binding protein. *Science* 268:1039–1041.
12. Wojtczak A, Cody V, Luft JR, Pangborn W (1996) Structures of human transthyretin complexed with thyroxine at 2.0 A resolution and 3′,5′-dinitro-N-acetyl-L-thyronine at 2.2 A resolution. *Acta Crystallogr D Biol Crystallogr* 52:758–765.
13. Hörnberg A, Eneqvist T, Olofsson A, Lundgren E, Sauer-Eriksson AE (2000) A comparative analysis of 23 structures of the amyloidogenic protein transthyretin. *J Mol Biol* 302:649–669.
14. Foss TR, Wiseman RL, Kelly JW (2005) The pathway by which the tetrameric protein transthyretin dissociates. *Biochemistry* 44:15525–15533.
15. Johnson SM, et al. (2005) Native state kinetic stabilization as a strategy to ameliorate protein misfolding diseases: A focus on the transthyretin amyloidoses. *Acc Chem Res* 38:911–921.
16. Colon W, Kelly JW (1992) Partial denaturation of transthyretin is sufficient for amyloid fibril formation in vitro. *Biochemistry* 31:8654–8660.
17. Hammarström P, Wiseman RL, Powers ET, Kelly JW (2003) Prevention of transthyretin amyloid disease by changing protein misfolding energetics. *Science* 299:713–716.
18. Liu K, Cho HS, Lashuel HA, Kelly JW, Wemmer DE (2000) A glimpse of a possible amyloidogenic intermediate of transthyretin. *Nat Struct Biol* 7:754–757.
19. Hurshman AR, White JT, Powers ET, Kelly JW (2004) Transthyretin aggregation under partially denaturing conditions is a downhill polymerization. *Biochemistry* 43:7365–7381.

20. Andersson K, Olofsson A, Nielsen EH, Svehag SE, Lundgren E (2002) Only amyloidogenic intermediates of transthyretin induce apoptosis. *Biochem Biophys Res Commun* 294:309–314.
21. Reixach N, Deechongkit S, Jiang X, Kelly JW, Buxbaum JN (2004) Tissue damage in the amyloidoses: Transthyretin monomers and nonnative oligomers are the major cytotoxic species in tissue culture. *Proc Natl Acad Sci USA* 101:2817–2822.
22. Sousa MM, Cardoso I, Fernandes R, Guimarães A, Saraiva MJ (2001) Deposition of transthyretin in early stages of familial amyloidotic polyneuropathy: Evidence for toxicity of nonfibrillar aggregates. *Am J Pathol* 159:1993–2000.
23. Bourgault S, et al. (2011) Mechanisms of transthyretin cardiomyocyte toxicity inhibition by resveratrol analogs. *Biochem Biophys Res Commun* 410:707–713.
24. Hammarström P, Jiang X, Hurshman AR, Powers ET, Kelly JW (2002) Sequence-dependent denaturation energetics: A major determinant in amyloid disease diversity. *Proc Natl Acad Sci USA* 99(Suppl 4):16427–16432.
25. Sekijima Y, et al. (2005) The biological and chemical basis for tissue-selective amyloid disease. *Cell* 121:73–85.
26. Jiang X, Buxbaum JN, Kelly JW (2001) The V122I cardiomyopathy variant of transthyretin increases the velocity of rate-limiting tetramer dissociation, resulting in accelerated amyloidosis. *Proc Natl Acad Sci USA* 98:14943–14948.
27. Coelho T, et al. (1996) Compound heterozygotes of transthyretin Met30 and transthyretin Met119 are protected from the devastating effects of familial amyloid polyneuropathy. *Neuromuscul Disord* 6:27.
28. Hammarström P, Schneider F, Kelly JW (2001) Trans-suppression of misfolding in an amyloid disease. *Science* 293:2459–2462.
29. Longo Alves I, Hays MT, Saraiva MJM (1997) Comparative stability and clearance of [Met30]transthyretin and [Met119]transthyretin. *Eur J Biochem* 249:662–668.
30. Adamski-Werner SL, Palaninathan SK, Sacchettini JC, Kelly JW (2004) Diflunisal analogues stabilize the native state of transthyretin. Potent inhibition of amyloidogenesis. *J Med Chem* 47:355–374.
31. Miller SR, Sekijima Y, Kelly JW (2004) Native state stabilization by NSAIDs inhibits transthyretin amyloidogenesis from the most common familial disease variants. *Lab Invest* 84:545–552.
32. Razavi H, et al. (2003) Benzoxazoles as transthyretin amyloid fibril inhibitors: Synthesis, evaluation, and mechanism of action. *Angew Chem Int Ed Engl* 42:2758–2761.
33. Wiseman RL, et al. (2005) Kinetic stabilization of an oligomeric protein by a single ligand binding event. *J Am Chem Soc* 127:5540–5551.
34. Connelly S, Choi S, Johnson SM, Kelly JW, Wilson IA (2010) Structure-based design of kinetic stabilizers that ameliorate the transthyretin amyloidoses. *Curr Opin Struct Biol* 20:54–62.
35. Kolstoe SE, et al. (2010) Trapping of palindromic ligands within native transthyretin prevents amyloid formation. *Proc Natl Acad Sci USA* 107:20483–20488.
36. Baures PW, Oza VB, Peterson SA, Kelly JW (1999) Synthesis and evaluation of inhibitors of transthyretin amyloid formation based on the non-steroidal anti-inflammatory drug, flufenamic acid. *Bioorg Med Chem* 7:1339–1347.
37. Baures PW, Peterson SA, Kelly JW (1998) Discovering transthyretin amyloid fibril inhibitors by limited screening. *Bioorg Med Chem* 6:1389–1401.
38. Choi S-W, et al. (2010) A substructure combination strategy to create potent and selective transthyretin kinetic stabilizers that prevent amyloidogenesis and cytotoxicity. *J Am Chem Soc* 132:1359–1370.
39. Green NS, Palaninathan SK, Sacchettini JC, Kelly JW (2003) Synthesis and characterization of potent bivalent amyloidosis inhibitors that bind prior to transthyretin tetramerization. *J Am Chem Soc* 125:13404–13414.
40. Johnson SM, Connelly S, Wilson IA, Kelly JW (2008) Toward optimization of the linker substructure common to transthyretin amyloidogenesis inhibitors using biochemical and structural studies. *J Med Chem* 51:6348–6358.
41. Johnson SM, Connelly S, Wilson IA, Kelly JW (2008) Biochemical and structural evaluation of highly selective 2-arylbenzoxazole-based transthyretin amyloidogenesis inhibitors. *J Med Chem* 51:260–270.
42. Klabunde T, et al. (2000) Rational design of potent human transthyretin amyloid disease inhibitors. *Nat Struct Biol* 7:312–321.
43. Oza VB, Petrassi HM, Purkey HE, Kelly JW (1999) Synthesis and evaluation of anthranilic acid-based transthyretin amyloid fibril inhibitors. *Bioorg Med Chem Lett* 9: 1–6.
44. Oza VB, et al. (2002) Synthesis, structure, and activity of diclofenac analogues as transthyretin amyloid fibril formation inhibitors. *J Med Chem* 45:321–332.
45. Petrassi HM, Klabunde T, Sacchettini J, Kelly JW (2000) Structure-based design of N-phenyl phenoxazine transthyretin amyloid fibril inhibitors. *J Am Chem Soc* 122: 2178–2192.
46. Hurshman Babbes AR, Powers ET, Kelly JW (2008) Quantification of the thermodynamically linked quaternary and tertiary structural stabilities of transthyretin and its disease-associated variants: The relationship between stability and amyloidosis. *Biochemistry* 47:6969–6984.
47. Hammarström P, Jiang X, Deechongkit S, Kelly JW (2001) Anion shielding of electrostatic repulsions in transthyretin modulates stability and amyloidosis: Insight into the chaotrope unfolding dichotomy. *Biochemistry* 40:11453–11459.
48. Schneider F, Hammarström P, Kelly JW (2001) Transthyretin slowly exchanges subunits under physiological conditions: A convenient chromatographic method to study subunit exchange in oligomeric proteins. *Protein Sci* 10:1606–1613.
49. Wiseman RL, Green NS, Kelly JW (2005) Kinetic stabilization of an oligomeric protein under physiological conditions demonstrated by a lack of subunit exchange: Implications for transthyretin amyloidosis. *Biochemistry* 44:9265–9274.
50. Wyman J, Gill SJ (1990) *Binding and Linkage: Functional Chemistry of Biological Macromolecules* (University Science Books, Mill Valley, CA).
51. Purkey HE, Dorrell MI, Kelly JW (2001) Evaluating the binding selectivity of transthyretin amyloid fibril inhibitors in blood plasma. *Proc Natl Acad Sci USA* 98: 5566–5571.
52. Purkey HE, et al. (2004) Hydroxylated polychlorinated biphenyls selectively bind transthyretin in blood and inhibit amyloidogenesis: Rationalizing rodent PCB toxicity. *Chem Biol* 11:1719–1728.
53. Sekijima Y, Dendle MA, Kelly JW (2006) Orally administered diflunisal stabilizes transthyretin against dissociation required for amyloidogenesis. *Amyloid* 13:236–249.
54. Blirup-Jensen S (2001) Protein standardization III: Method optimization basic principles for quantitative determination of human serum proteins on automated instruments based on turbidimetry or nephelometry. *Clin Chem Lab Med* 39:1098–1109.
55. Lashuel HA, Hartley D, Petre BM, Walz T, Lansbury PT, Jr. (2002) Neurodegenerative disease: Amyloid pores from pathogenic mutations. *Nature* 418:291.
56. Bartalena L, Robbins J (1993) Thyroid hormone transport proteins. *Clin Lab Med* 13: 583–598.
57. Rosen HN, Moses AC, Murrell JR, Liepnieks JJ, Benson MD (1993) Thyroxine interactions with transthyretin: A comparison of 10 different naturally occurring human transthyretin variants. *J Clin Endocrinol Metab* 77:370–374.
58. Holmgren G, et al. (1992) Homozygosity for the transthyretin-Met30-gene in seven individuals with familial amyloidosis with polyneuropathy detected by restriction enzyme analysis of amplified genomic DNA sequences. *Clin Genet* 41:39–41.
59. Coelho T, et al. (2012) Tafamidis for transthyretin familial amyloid polyneuropathy: A randomized, controlled trial. *Neurology*, in press.
60. Cody V, Wojtczak A (2009) Mechanisms of molecular recognition:structural characteristics of transthyretin ligand interactions. *Recent Advances in Transthyretin Evolution, Structure and Biological Functions*, eds Richardson SJ and Cody V (Springer, Berlin), pp 1–21.